ELSEVIER

Journal of Molecular Catalysis A: Chemical 98 (1995) 25–34

JOURNAL OF MOLECULAR CATALYSIS A: CHEMICAL

Oxidative coupling of methane over natural manganese oxide

L.M. Ioffe [1], T. Lopez, Y.G. Borodko [1,*], R. Gomez

Universidad Autonoma Metropolitana-Iztapalapa, Department of Chemistry, A.P. 55-534 Mexico D.F. 09340, Mexico

Received 13 June 1994; accepted 7 November 1994

Abstract

Oxydehydrogenative coupling of methane to higher hydrocarbons has been achieved with high selectivity towards C_2 products over natural mineral manganese oxides. Oxide treatments under hydrocarbon atmosphere show that the reduction of manganese ions Mn(IV), Mn(III) to Mn(II) is mainly responsible for the catalyst deactivation. The tests using $CH_4 + CD_4$ equimolecular mixtures and the analysis of the $(HD)C_2$ products by cryospectroscopic IR showed that ethane is the primary product. No evidence of CH_2 species in the gas phase was observed.

Keywords: Ethane; IR spectroscopy; Isotopic methane; Manganese catalysts; Methane; Oxidative coupling

1. Introduction

The oxidative dehydroogenation of methane to C_2 or to higher hydrocarbons is an interesting reaction for the use on the reserve of natural gas. A large number of catalysts have been reported as successful for the oxidative coupling of methane [1–3]. Of the reducible oxides, manganese oxide has shown to be a promising catalyst. The selectivity towards C_2 products increased markedly after modification of individual manganese oxides with alkali and alkali–earth elements [4–7]. Manganese oxide catalysts usually operate in redox mode. Inasmuch as manganese oxide is a stoichiometric reagent in the redox approach to methane conversion, since the way to increase methane conversion is to increase manganese loading. Jones et al. [4,5] found that the optimum manganese loading is close to 15–20 wt%. In this connection, natural manganese mineral (NMM) with high content of manganese oxide (15–35 wt%) was used as a base for preparing the catalysts for the oxidative coupling of methane (OCM). The starting material is essentially different from synthetic manganese minerals such as manganite, psilomelane and pyrolusite. Besides manganese oxides, NMM includes a number of other elements and compounds: Na, Mg, Ba, Ca, Al_2O_3 and SiO_2 which can be considered as chemical and structural promoters.

Alkali–phosphorus-promoted NMM oxides have been prepared and tested for oxidative coupling of methane. The catalyst was characterized by ESCA and IR spectroscopies. Activities and selectivities were studied in the OCM reaction. $CH_4 + CD_4$ were used as reactants, and the mechanism of the reaction was followed by the analysis of the IR absorption spectra of the deuterated C_2 products.

* Corresponding author.

[1] On leave of absence from Institute of Chemical Physics, Russia.

SSDI 1381-1169(94)00079-4

2. Experimental

2.1. Catalyst preparation

Natural manganese ore samples from Nikopol field, Ukraine were obtained from the Dnepropetrovsk Mining Institute. The typical composition of manganese ore concentrate was (in wt%): MnO_2, 28; Mn_2O_3, 8; Fe_2O_3, 4; FeO, 1; K_2O, 3; Na_2O, 1; CaO, 2; MgO, 1; BaO, 1; SiO_2, 27; Al_2O_3, 7; SO_3, 1; P_2O_5, 0.5; C, 8; others 7.

Before the catalytic test, the samples with manganese oxide contents of 20–25 wt% were calcined for 16 h at 800°C in air and then they were impregnated with a dilute solution of $Na_4P_2O_7$ until the content of sodium pyrophosphate reached 5 wt%. After that the impregnated samples were calcined at 800°C in air for 16 h. The results of surface analysis of NMM materials by XPS technique are presented in Table 1.

2.2. X-ray photoelectron and Auger characterization

Surface characterization was performed in an ESCA spectrometer Physical Electronics PHI-551 with base pressure of 2×10^{-8} Pa using a MgKα X-ray source. To compensate for possible charging effects, binding energies have been normalized with respect to the position of the C 1s line for the contaminated carbon. The latter was held constant at 285 eV.

Table 1
Surface analysis of NMM materials

Element	Term	Surface contents (at%)		
		Initial NMM	NMM calcined [a]	$Na_4P_2O_7$/NMM calcined [a]
Mn	2p	10.2	14.8	11.5
Ca	2p	1.4	2.3	2.0
K	1s, 2p	0	0.4	2.7
Na	1s, 2p	0.1	0.1	0.4
Si	2s, 2p	4.0	8.4	14.3
P	2p	0	1.1	4.0
O	1s	40.0	53.0	52.0
C	1s	44.6	20.0	13.7

[a] Calcined in air for 16 h at 800°C.

2.3. Catalytic experiments

The catalytic experiments were performed in redox approach to methane conversion in a quartz fixed-bed flow reactor (40 cm × 8 mm I.D.) operated under atmospheric pressure at 850°C. The reactor tubes were heated to reaction temperature under a flow of air. After one experiment run the reduced NMM catalyst was regenerated with air at reaction temperature. In a typical redox sequence the air was purged from the reactor with argon before the methane sequence began. Methane conversion runs were typically of 1 to 2 min in length. The reactor residence time was modified by varying the flow rate. A catalyst mass of 4.5 g was used in all the experiments. Cumulative product of 1 min flow was collected and analyzed by a gas chromatograph apparatus equipped with thermal conductivity and flame ionization detectors using Porapak-Q and molecular sieve packed columns. The sum of ethane, ethylene, carbon monoxide and carbon dioxide was used to calculate the methane conversion.

2.4. IR characterization

IR spectra were recorded with Perkin Elmer 325 spectrophotometer. The preliminary oxidized (fresh) catalyst samples were put in a quartz vessel and calcined at 850°C in oxygen, air, methane, ethane, ethylene or in vacuum. The sample of catalyst after the treatment was cooled to room temperature in a reactive atmosphere and then the KBr pellet with catalyst was formed in the air.

The cumulative product of oxidative coupling of $CH_4 + CD_4$ mixture was separated with chromatograph. (HD)ethanes and (HD)ethylenes were gathered using cooling traps as collecting box. For the study of the gaseous products at room temperature an optical gas cell was used, while for the study of frozen C_2 products a cryospectroscopic reflection–absorption cell maintained at −190°C was used.

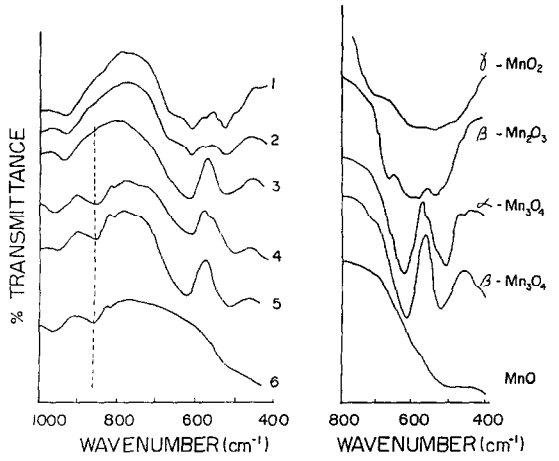

Fig. 1. IR absorption spectra of manganese oxide catalysts (left side) after calcination at 850°C for 60 min in: (1) oxygen, (2) argon, (3) vacuum, (4) methane, (5) ethane, 30 min, (6) ethane, 60 min. Right side, manganese oxide reference spectra.

3. Results

3.1. Effect of oxidizing and reducing treatments on the chemical state of the catalysts

The IR spectra of the catalysts pretreated under different atmospheres are shown in Fig. 1 and compared with those of some well known manganese oxides. First of all, after oxidizing in oxygen atmosphere for 1 h the catalyst mainly consists of MnO_2 and Mn_2O_3 oxides. The oxidized catalyst is rather stable in Ar atmosphere at high temperature. Under these conditions it does not lose lattice bulk oxygen substantially. Dramatic changes, however, were observed when the catalyst was treated in vacuum or hydrocarbon atmospheres. Manganese oxides with manganese states Mn(IV) and Mn(III) were reduced to low oxidation state. On the basis of the IR results the conclusion may be drawn that the ability of reducing bulk manganese oxides in NMM is as follows: ethane > methane > vacuum annealing. The reduction of manganese oxides by methane in OCM reaction was observed earlier in the case of MnO_x/SiO_2 catalyst [8].

It is necessary to note that the formation of the 'bulk' carbonate take place simultaneously with reducing manganese oxides under hydrocarbon atmosphere. The strong absorption band which appears at 860 cm^{-1} is characteristic of CO_3^{2-} carbonate vibration ν_2 (A_2'') [9]. The carbonate observed is rather stable at high temperature and is not sensitive to the oxidative state of manganese.

The chemical composition of surface carbonaceous material changes markedly after a redox cycle, as shown by the comparison between the shape of C 1s carbon lines in the X-ray photoelectron spectra for fresh and used catalysts. In XPS spectrum of fresh catalyst the C 1s line contains a high energy shoulder with binding energy at 288 eV, which is attributed to carbon in CO_3^{2-} group (Fig. 2C). In addition, in the spectrum of the catalyst used (Fig. 2D) a new line in the low energy side with binding energy at 282.5 eV appears. This line can be assigned to CH_x species on the surface of the catalyst.

The comparison the data obtained with IR and XPS spectroscopies have shown, that on the one hand, in static condition, the formation of the bulk carbonate phase takes place during heating of NMM catalyst in hydrocarbon atmosphere for 60 min and on the other hand, the decrease of the

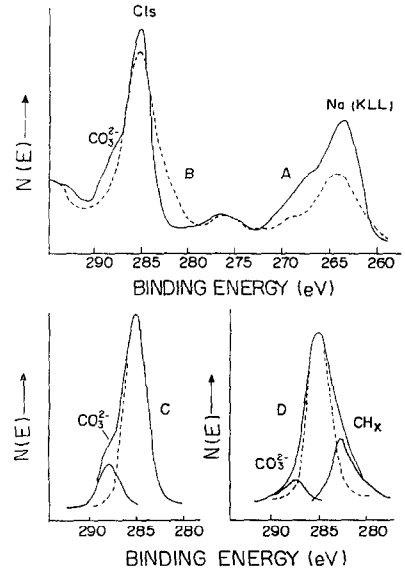

Fig. 2. X-ray photoelectron spectra of carbon C 1s and Auger spectra of sodium Na (KLL) for: (A) fresh manganese oxide catalyst oxidized at 850°C in air for 30 min; (B) catalyst (sample A) after one run OCM experiment; (C) XPS spectrum of carbon C 1s for sample A background corrected and deconvoluted; (D) XPS spectrum of C 1s of sample B background corrected and deconvoluted.

Table 2
Redox runs over manganese oxide and data after ref. [7,12]

Catalyst	Feed gas	GHSV h^{-1}	Conversion CH_4, %	Selectivity (%)				Yield C_2 (%)	Ref.
				C_2	C_2H_6	C_2H_4	CO_x		
NMM	CH_4	7300	11	86	30	56	14	9.5	
NMM	CH_4	11400	9	97	42	55	3	8.7	
NMM	CH_4+CHCl_3	11400	24	82	9	73	18	20.0	
NMM [a]	CH_4	6200	27	80	9	71	20	22.0	
15%Mn $5\%Na_4P_2O_7/SiO_2$	CH_4	860	22	77 [b]	4	47	22	17.0 [b]	[12]
10%Mn, 1.7%Na on SiO_2	CH_4	860	6	91 [b]					[12]
10%Mn, 1.7%Na on SiO_2	CH_4	860	12	88 [b]					[12]
MnO_2	CH_4+O_2 [c]		46.8	10.9	7.3	3.6	89	5.1	[7]
MnO/SiO_2	CH_4+O_2		8.4	13.6	11.5	2.1	86.4	1.1	[7]
$NaCl/MnO_2$ on SiO_2	CH_4+O_2		16.7	82.5	31.2	51.3	17.5	13.8	[7]

[a] The catalyst was treated with chloroform.
[b] C_{2+} selectivity and yield of C_{2+} after ref. [12].
[c] Initial activities and selectivities, $CH_4:O_2=20:1$, after ref. [7].

'surface' carbonate takes place during 1 min run of OCM reaction. It testified in favour of absorption of CO_2 by NMM catalyst in the case of the prolonged static experiments and against CO retention by the catalyst during 1 min OCM run.

In order to estimate the degree of coke formation, the catalyst was purged with oxygen at reaction temperature after one OCM experiment run and the effluent was examined by chromatography. A trace of CO_2 was found only. If the used catalyst was purged with argon at reaction temperature traces of CO_2, CH_4 and C_2 products were found.

Surface analysis showed that the amount of carbonaceous material is negligible on the catalyst surface after one OCM experiment run. As can be seen from Fig. 2, the ratio of the intensities of C 1s carbon line (binding energy at 285 eV) and Auger Na(KLL) line (264 eV) changes from [C]/[Na] = 1.7 to [C]/[Na] = 3. These data may be used to evaluate the thickness of the CH_x film on the surface of the NMM catalyst. It can be determined from the relation for two XPS line [10] (with close energy). One of them (I_C) refers to the overlayer CH_x and second one (I_{Na}) refers to the sub-surface of the NMM catalyst.

$$I_C/I_{Na} = N_C\lambda_C/N_{Na}\lambda_C * [1-\exp(-d/\lambda_C)]/\exp(-d/\lambda_C)$$

where N is the atomic density, $\lambda(E)$ is inelastic mean free path and d is the thickness of the overlayer. Suppose that the values of N and λ are identical in both cases, but the thickness of the deposited carbonaceous film changed from d for the fresh catalyst to the meaning $d+\Delta$ for used catalyst. Quantity of Δ is characteristic of the additional CH_x carbonaceous layer which formed during the OCM run and it is responsible for the change of I_C/I_{Na} ratio. In such approach Δ is equal to 6–8 A° if the value of $\lambda = 10$ Å [21]. The low carbon deposition found and the high reducibility observed on the manganese oxide catalyst, allow us to suggest that deactivation must be mainly caused by the reduction of Mn(IV) and Mn(III) to Mn(II).

3.2. Activity and selectivity of catalysts

The results of one run experiment in redox mode are presented in Table 2. As can be seen, the activity of natural manganese oxide catalysts is comparable with the activity of the synthetic manganese oxide catalysts [7,12].

The high selectivity to C_2 hydrocarbons is especially remarkable regarding the complex composition of the NMM catalysts. The composition of C_2 products substantially depends on the methane

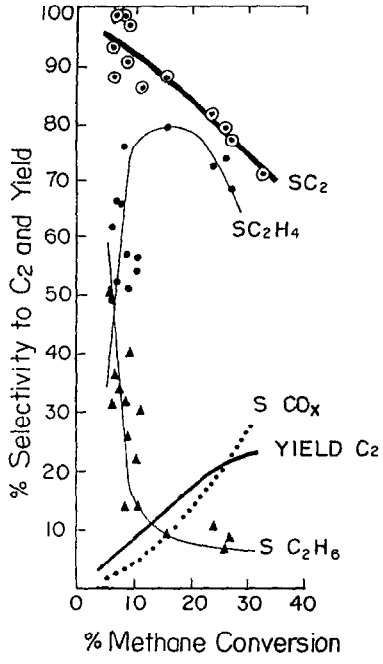

Fig. 3. Conversion–selectivity (S) relationships for the oxidative coupling of methane over manganese oxide catalysts under investigation (redox cycle).

conversion: at low conversion the amount of ethane was higher than the amount of ethylene.

The effect of the introduction of gas-phase chlorine-containing additives in the methane conversion process has been shown previously [6,11]. In the case of NMM catalyst, the distribution of C_2 products is markedly changed by cofeeding a small quantity of $CHCl_3$ as a source of chlorine. As shown in Table 2, at equal value of GHSV (11400) the ethane and ethylene selectivities differ considerably. If the feed gas was only methane, the ratio $[C_2H_6]/[C_2H_4]$ was 1:1.3, when the feed gas was $CH_4 + CHCl_3$ (5 vol%) the $[C_2H_6/C_2H_4]$ ratio reached 1:8. In all probability, $CHCl_3$ establishes an additional route for the coupling reaction, presumably by creating new active sites

Table 3
Redox runs of $CH_4 + CD_4$ over NMM catalyst

Feed gas	GHSV h^{-1}	Conversion (%) $CH_4 + CD_4$	Selectivity (%)		
			C_2H_6	C_2H_4	CO_x
$CH_4 + CD_4$	620	25	8	67	25
$CH_4 + CD_4$	16000	3	83	16	1

or by modifying existing sites on the catalyst surface (for example, surface oxy-chlorine species) The NMM catalyst possess a long-term 'memory' concerning the use of chloroform as gas-phase additive. If NMM catalyst have interacted with methane–chloroform mixture (for 1–2 min) and then it was used again in OCM run with CH_4 only (after the following reoxidation and purgation at reaction temperature) the conversion and selectivity to C_2 products were very close to the findings of the experiments with chloroform as gas-phase additive (Table 2). The data obtained are summarized in Fig. 3.

As far as catalyst deactivation is concerned, it is noteworthy that the NMM catalyst is very stable to overheating: when it was calcined for 1–3 h at 1200°C in air, its activity and selectivity diminish in the OCM reaction by less than 10%.

3.3. IR spectroscopy study

In order to carry out spectroscopic analysis of isotopic C_2 products of the oxidative coupling of equimolecular $CH_4 + CD_4$ mixture, two sets of reaction products have been synthesized: at low (3%) and high (25%) methane conversion (Table 3). It was established that the value of H–D exchange between CH_4 and CD_4 is insignificant at low methane conversion.

In order to obtain experimentally more reliable data about the composition of $(HD)C_2$ products, the mixtures of (HD)ethanes, only, and (HD)ethylenes, only, were recorded in the solid (frozen) state. It eliminates the rotational structure of vibrational bands and induces the appearance of narrow Q branches and thus improves the precision of spectral analysis.

The IR spectroscopic analysis of frozen $(HD)C_2$ hydrocarbons has the advantage over IR and mass-spectral measurements in the gaseous state. All deuterated ethylenes and ethanes are characterized by well resolved absorption bands in solid state.

As illustrated in Fig. 4, the original broad rotation–vibration structure of vibrations of gaseous ethane and ethylene disappears in solid state. For

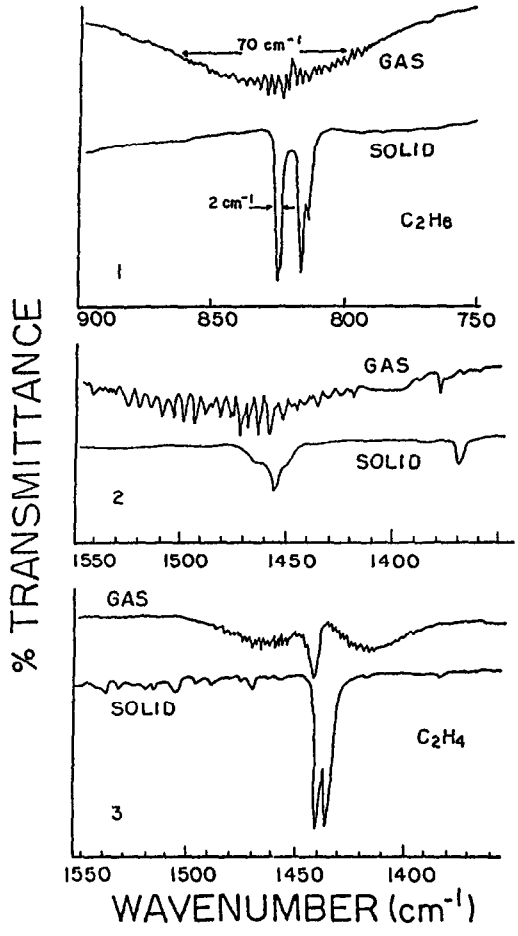

Fig. 4. IR spectra of solid (frozen at −190°C) and gaseous (1) ethane, (2) ethane: (3) ethylene.

example the width (FWHM) of the C–C bending vibration of ethane at 830 cm^{-1} decreases from 70 cm^{-1} in gas phase to 2 cm^{-1} in solid state. Apart from the disappearance of the rotational structure in IR spectra of C_2 products frozen at low temperature, it is necessary to take into account the possibility of the spectra displaying other phenomena, such as: (i) ⟨gas–solid⟩ band shift; (ii) the appearance of vibrational-band fine-structure splitting as a result of the crystal-field effect.

Such an effect can be seen distinctly in Fig. 4. Fortunately, this phenomenon did not affect the interpretation of data obtained.

As illustrated in Fig. 5, the spectrum of (HD)ethanes in solid state is more informative than the corresponding one in gaseous state. In the case of high methane conversion the IR spectrum contains a full set of absorption bands, which are assigned to the isotopic enhances: d_0, d_1, d_2, d_3, d_4, d_5 and d_6 (Fig. 5 B). It should be noticed, that apart from the frequencies of (HD)ethanes listed in Table 4, a number of the additional bands (733, 686 cm^{-1}) was observed in the spectrum of (HD)ethanes at high conversion of methane, which may be assigned to H_3CCHD_2 (d_2) and H_2DCCHD_2 (d_3). The positions of ν CCH(D) bending vibrations calculated theoretically are presented at the bottom of the picture as sharp 'islands'. As one can see there is a good correlation between the experimental and theoretical data.

At low methane conversion only three isotopes: H_3CCH_3, H_3CCD_3, D_3CCD_3 (d_0, α-d_3, d_6) were observed in the spectrum of the frozen products (Fig. 5 D). A very similar result was obtained for the composition of the (HD)ethylene products of the oxidative coupling of the equimolecular mixture $CH_4 + CD_4$ (Fig. 6).

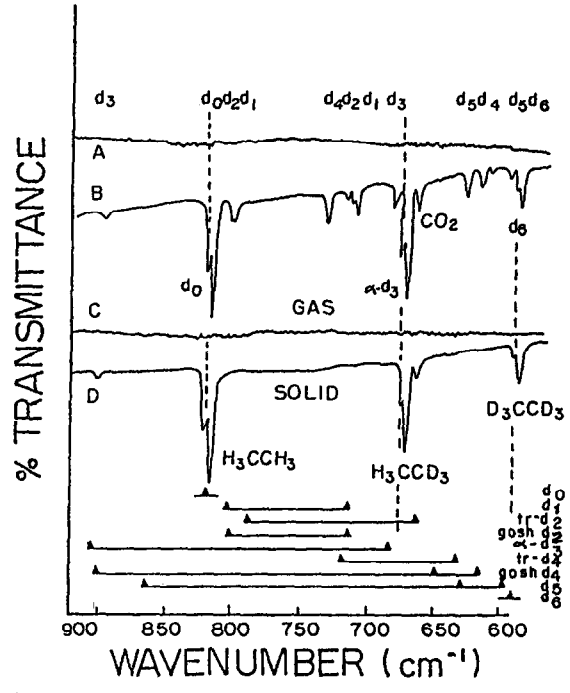

Fig. 5. IR spectra of (HD)ethanes: (A) gaseous, 25% methane conversion; (B) sample A in solid state at −190°C; (C) gaseous, 3% methane conversion; (D) sample C in solid state at −190°C.

At 25% methane conversion, all deuterated ethylenes have been identified in the spectrum of the products, but noticeable amounts of the isotopes H_2CCH_2, H_2CCD_2, and D_2CCD_2 were exhibited for the conversion of the 3% (CH_4+CD_4) mixture. The experimental position of the IR bands ν_{max} of solid (HD)ethanes and (HD)ethylenes are summarized in Table 4, as well as the theoretically calculated vibrations for gaseous (HD)C_2-isotopic molecules [13].

The concentration distribution of the ethanes: d_0, α-d_3, d_6 reflects the relative concentration of $CH_3^{\cdot}$ and $CD_3^{\cdot}$ determined by the kinetic isotope effect. We attempted to estimate the concentration ratio of isotopic (HD)ethanes using the values of integral intensity for gaseous molecules from literature data [13–15] and suitable (our own) data obtained for individual solid C_2D_6 and C_2H_6. Rough estimation of the concentration ratio $[H_3CCH_3]:[H_3CCD_3]:[D_3CCD_3]$ at low methane conversion was determined by IR spectroscopy as 1.7:2.7:1 respectively, and it reflects a kinetic isotope effect in methyl radical formation.

The concentration ratio d_0:α-d_3:d_6 of the ethanes was calculated also based on kinetic isotope

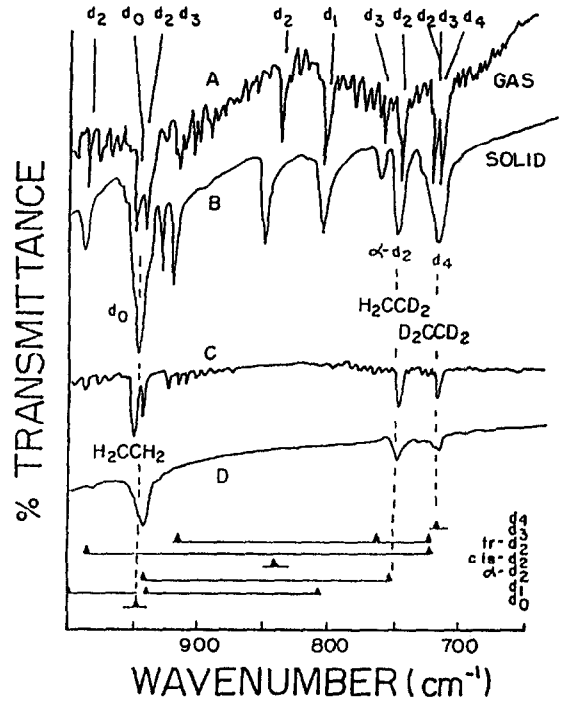

Fig. 6. IR spectra of (H–D)ethylenes: (A) gaseous, 25% methane conversion; (B) sample A in solid state at −190°C; (C) gaseous, 3% methane conversion; (D) sample C in solid state at −190°C.

effect, k_H/k_D (1.2–1.5) in methyl radical formation and statistical distributions of isotopic ethanes

Table 4
IR spectra of gaseous and solid labelled (HD)ethylenes and (HD)ethanes, cm^{-1}

Ethylenes	[a]	ν_2, C–H(D) bending		ν_7, C–H(D) out-of-plane		Ethanes	[a]	ν CCH(D) bending	
		gas	solid	gas	solid			gas	solid
C_2H_4	d_1	1444	1438	949	947	C_2H_6	d_0	821	819
C_2H_3D	d_1	1403	1396	807	808	C_2H_5D	d_1	715	714
								806	805
H_2CCD_2	α-d_2	1384	1378	742	753	*trans*-$(CH_2D)_2$	d_2	791	
cis-$(CHD)_2$	d_2	1342	1336	842	852	gauche $(CH_2D)_2$	d_2	715	716
								805	803
trans-$(CHD)_2$	d_2	1300	1295	727	735	H_3CCD_3	α-d_3	685	680
									676
C_2HD_3	d_3	1290	1283	724	726	*trans*-$(CHD_2)_2$	d_4	635	631
								720	720
C_2D_4	d_4	1078	1073	720	721	gauche $(CHD_2)_2$	d_4	618	620
								651	
						C_2HD_5	d_5	599	599
								631	631
						C_2D_6	d_6	594	594
									592

ν gas, calculated theoretically [13,14]; ν solid, determined experimentally in this work.
[a] Number of deuterium atoms in molecule.

Table 5
Concentration ratio $[D_3CCD_3]:[H_3CCD_3]:[H_3CCH_3]$ versus value of kinetic isotope effect (k_H/k_D) in methyl radical formation

k_H/k_D	D_3CCD_3	H_3CCD_3	H_3CCH_3
1.2	1	2.53	1.57
1.3	1	2.7	1.86
1.4	1	2.94	2.15
1.5	1	3.16	2.47

at given KIE within the framework of collision theory. We assumed that every collision of CH_3 and CD_3 radicals results in ethane formation with activation energy close to zero. The number of collisions Z per volume unit per time unit was estimated from the following equations [16]:

$$Z_{AA} = \pi d^2 (4kT/\pi m)^{1/2} (N/V)^2 \qquad \begin{matrix} CH_3^{\cdot} \cdots CH_3^{\cdot} \\ CD_3^{\cdot} \cdots CD_3^{\cdot} \end{matrix}$$

$$Z_{AB} = \pi d^2 (8kT/\pi\mu)^{1/2} (N_A N_B/V^2) \qquad CH_3^{\cdot} \cdots CD_3^{\cdot}$$

The data calculated are shown in Table 5. The comparison between the experimental and the calculated data shows that the distribution of (HD)ethanes in products at low methane conversion corresponds to the value of $k_H/k_D = 1.3$.

4. Discussion

The activity and selectivity of the catalysts based on natural manganese minerals in the reaction of the oxidative coupling of methane are very close to those prepared with synthetic manganese oxide catalysts [4–7,12] at high manganese oxide content (20–25 wt%). It confirms to the so-called 'Boreskov' rule, which states that independently of the preparation method of the catalyst, at high temperature, the catalyst properties in stationary state depend, mainly, on the composition. The overall mechanism of methane activation reaction is probably similar for both synthetic modified MnO_x catalyst and NMM catalyst.

The mechanism of the methane oxidative coupling is currently under consideration, especially as far as the nature of primary intermediate species and C_2 hydrocarbons is concerned [1–3,17]. At present, a few reaction routes for oxidative coupling of CH_4 to C_2 hydrocarbons are under consideration. They involve $CH_3^{\cdot}$ and CH_2 radicals as primary species [1].

To obtain the information about the primary C_2 hydrocarbons, the products of the oxidative coupling of $CH_4 + CD_4$ equimolecular mixture [18] over NMM catalysts were studied. For the first time conversion of $CH_4 + CD_4$ mixture in OCM reaction was studied in the seminal work of Nelson and Cant [19]. They have studied the mixture of gaseous (HD)C_2 products in OCM reaction over Li/MgO, $SrCO_3$ and Sm_2O_3 catalysts and have showed that the participation of methylene radicals in this systems is not significant.

To avoid some ambiguity in the quantitative estimation of gaseous (HD)ethanes amounts by IR spectroscopy we used for the first time the cryospectroscopic technique to determine the composition and the structure of (HD)ethanes and (HD)ethylenes separately [20].

If $CH_3^{\cdot}$ radicals are produced on the surface of the catalyst and then released into the gas phase, they dimerize to yield ethane as the primary C_2 product. If ethylene is produced by gas-phase conversion of ethane, in this case the formation of C_2 products may be described by the reaction sequence (Scheme 1) and relative concentrations of d_0, α-d_2 and d_4 ethylenes would not be significantly different from that of the ethanes [19].

If, along with $CH_3^{\cdot}$ radicals, carbene species CH_2 are produced on the surface of the catalyst and methylene species are released to the gas phase, then the whole set of (HD)ethanes arises in gas phase, as shown in Scheme 2.

The data obtained show that at low conversion of the equimolecular mixture $CH_4 + CD_4$ over the natural manganese mineral catalyst only three isotopic ethanes: d_0, α-d_3, d_6 and three isotopic ethylenes: d_0, α-d_2, d_4 were produced with the very

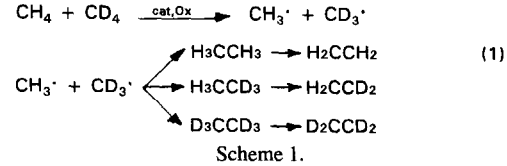

Scheme 1.

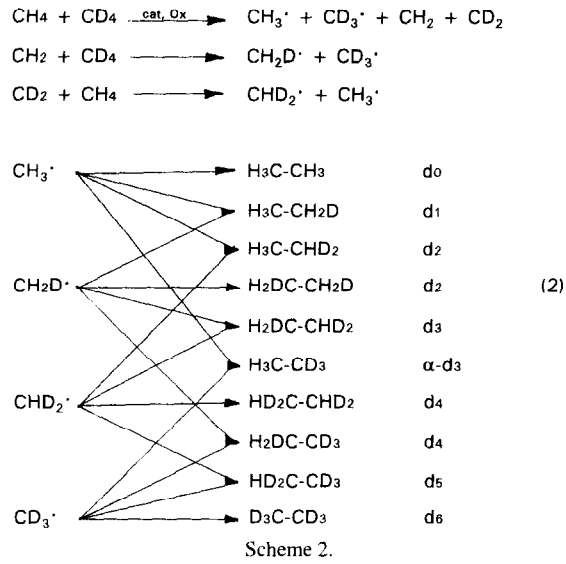

Scheme 2.

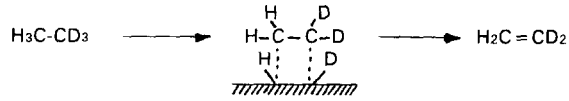

Scheme 3.

close distribution of respective deuterated molecules.

This fact suggests that:

(i) ethane is the primary product, and the result of the recombination of methyl radicals in gas phase;

(ii) probably, ethylene is produced by gas-phase conversion of ethane and/or oxidative remote of two hydrogen atoms on the surface (Scheme 3). (However, the this supposition is less reliable, since in this case H–D exchange and appearance of different (HD)ethanes are more probable.);

(iii) no evidence of carbene species $CH_2(CD_2)$ was detected in the gas phase.

At high methane conversion (more prolonged residence time) all (HD)ethanes and (HD)ethylenes were detected. It may be connected with the following:

(i) CH_2 (CD_2) species can be formed on the surface and then released to the gas phase.

(ii) at high residence time, substantial secondary H–D exchange between the hydrocarbons takes place.

5. Conclusions

Natural manganese minerals are interesting materials which can be used as starting material for the preparation of selective catalysts for the oxidative coupling of methane. These catalysts possess high temperature stability and long stability in the OCM reaction. IR and ESCA studies show that in NMM catalysts the manganese oxidation state is strongly modified to low oxidation states when the materials are treated under hydrocarbon atmosphere.

Investigation of the oxidative coupling of a $CH_4 + CD_4$ equimolecular mixture over catalysts based on natural manganese minerals shows that at low methane conversion, (HD)ethanes are the primary products of dimerization of CH_3 and CD_3 radicals in gas phase.

An IR cryospectroscopic method was developed for analysis of frozen $(HD)C_2$ products of oxidative coupling of $CH_4 + CD_4$ mixture and was applied for the first time to study the composition and structure of all $(HD)C_2$ hydrocarbons formed in the OCM reaction.

Acknowledgements

The authors are pleased to acknowledge Prof. P.Bosch for valuable discussions and Dr. V.I. Rubzov for experimental assistance in the measurements of the ESCA spectra. We are also indebted to CONACYT-México and to the Academy of Sciences of Russia for their financial support.

References

[1] G.J. Hutchings, M.S. Scurrell and J.R. Woodhouse, Chem. Soc. Rev., 18 (1989) 251.

[2] Y. Amenomiya, V.I. Birss, M. Goledzinowski, J. Galuszka and A.R. Sanger, Catal. Rev.-Sci. Eng., 32 (1990) 163.

[3] A.M. Maitra, Appl. Catal. A, 104 (1993) 11.

[4] J.A. Sofranko, J.J. Leonard and C.A. Jones, J. Catal., 103 (1987) 302.

[5] C.A. Jones, J.J. Leonard and J.A. Sofranko, Energy Fuels, 1 (1987) 12.

[6] K. Otsuka, K. Jinno and A. Morikawa, Chem. Lett., 5 (1985) 467; K. Otsuka and T. Komatsu, J. Chem. Soc., Chem. Commun., 5 (1987) 388.
[7] R. Burch, G.D. Squire and S.C. Tsang, Appl. Catal., 43 (1988) 105.
[8] J.M. Fox, T.P. Chen and B.D. Degen, Chem. Eng. Progr., 86 (1990) 42.
[9] K. Nakamoto, Infrared and Raman Spectra of Inorganic and Coordination Compounds, J. Wiley and Sons, 1978.
[10] J.W. Niemantsverdriet, Spectroscopy in Catalysis, VCH, Weinheim, 1993, p. 56; W. Hirschwald, in J. Nowotny and L.-C. Dufour (Eds.), Surface and Near-Surface Chemistry of Oxide Materials, Materials Science Monographs, Vol. 47, Elsevier, Amsterdam, 1988; T.N. Rhodin and G. Ertl (Eds.), Electron Spectroscopy and the Surface Chemical Bond, North-Holland, 1984, p. 173.
[11] S. Ahmed and J.B. Moffat, J. Catal., 125 (1990) 54; D.I. Bradshaw, P.T. Cooler, R.W. Jadd and C. Komodromos, Catal. Today, 6 (1990) 427.
[12] C.A. Jones, J.J. Leonard and J.A. Sofranko, J. Catal., 103 (1987) 311.
[13] L.M. Sverdlov, M.A. Kovner and E.P. Krainov, Vibrational Spectra of Polyatomic Molecules, New York, Wiley, 1973.
[14] S. Pinchas and I. Laulicht, Infrared Spectra of Labelled Compounds, Academic Press, New York, 1971.
[15] A.J Barnes and W.J. Orville-Thomas (Eds.), Vibrational Spectroscopy Modern Trends, Elsevier, Amsterdam, 1977.
[16] P.W. Atkins, Physical Chemistry, W.H. Freeman and Co., New York, 1982.
[17] J.H. Lunsford, Stud. Surf. Sci. Catal., 75(A) (1993) 103.
[18] L. Melander and W.H. Sauders, Jr., Reaction Rates of Isotopic Molecules, J. Wiley and Sons, New York, 1980.
[19] P.F. Nelson, C.A. Lukey and N.W. Cant, J. Phys. Chem., 92 (1988) 6176; J. Catal., 120 (1989) 216.
[20] Y.G. Borodko, L.M. Ioffe, A.Y. Borodko Jr., Catal. Today, 13 (1992) 549.
[21] M.P. Seah and W.A. Dench, Surf. Interface Anal., 1 (1979) 2. S. Tanuma, C.J. Powell and D.R. Penn, Surf. Interface Anal., 20 (1993) 77